Presence of electrolyte promotes wetting and hydrophobic gating in nanopores with residual surface charges†

Laura Innes,[a] Diego Gutierrez,[a,b] William Mann,[a,b] Steven F. Buchsbaum[a] and Zuzanna S. Siwy*[a,c,d]

Hydrophobic nanopores provide a model system to study hydrophobic interactions at the nanoscale. Such nanopores could also function as a valve since they halt the transport of water and all dissolved species. It has recently been found that a hydrophobic pore can become wetted *i.e.* filled with condensed water or an aqueous solution of salt when a sufficiently high electric field is applied across the membrane. The wetting process is reversible thus when the voltage is lowered or switched off, the pore comes back to a closed state due to water evaporation in the pore. In this manuscript we present experimental studies on how the switching between conducting and non-conducting states can be regulated by the electrolyte concentration. Transport properties of single nanopores modified with alkyl chains of different lengths were recorded in salt concentrations between 10 mM and 1 M KCl. Nanopores modified with propyl chains exhibited gating in 10 mM KCl and were open for ionic transport for all voltages at higher salt concentrations. Nanopores modified with decyl chains did not conduct current in 10 mM and exhibited repeatable hydrophobic gating in 100 mM and 1 M KCl. The results are explained in the context of Maxwell stress in confined geometry with local surface charges, which change the shape of the water–vapor interface and promote wetting.

Introduction

There has been a lot of interest in creating nanoporous structures which, similar to biological channels in a cell membrane, could regulate water, ionic, and molecular transport.[1–6] Control of transport by hydrophobic interactions is especially interesting, since a hydrophobic nanopore provides the means to regulate the transport of water and therefore any species which is dissolved in it. Water and ions permeate such a pore only if sufficiently high external stimulus, *e.g.* pressure difference, is applied. Moreover, hydrophobic interactions at the nanoscale make the system reversible so that when the stimulus is removed water in a hydrophobic nanopore undergoes spontaneous evaporation halting all transmembrane transport. Hydrophobic systems could therefore become the basis for

on-demand drug delivery systems, nonlinear circuits, and biosensors.[3]

A great deal of research has been done on understanding sorption/desorption of water in nanopores and on hydrophobic surfaces as a function of applied pressure.[7–9] An existence of hysteresis was found such that the pressure needed to cause sorption of water, leading to pore wetting, is higher than the pressure needed to cause desorption.[1,7,9] This observation is in agreement with the hysteresis of a contact angle *i.e.* the advancing angle is larger than the receding angle.[10] Experimental and modeling studies also showed that with the increase of surface hydrophobicity, seen as the increase of contact angle, the sorption pressure increases leading to widening of the hysteresis.[7]

When the pore opening approaches truly nanometer dimensions, the pressures required to wet a hydrophobic pore become very high thus making such pressure-driven systems very difficult to build and operate.[1,11] High electric fields on the other hand can be applied across membranes without the necessity of mechanically strengthening the system. Electric fields were indeed found to open hydrophobic pores for water and ionic transport.[11–13] Electric field induced transition of wetting/dewetting is typically examined in a form of current–voltage curves. When a pore or its section is filled with vapor

[a]Department of Physics and Astronomy, University of California, Irvine, CA 92697, USA. E-mail: zsiwy@uci.edu; Tel: +949-824-8290
[b]Department of Physics, California State University, Long Beach, CA, USA
[c]Department of Chemistry, University of California, Irvine, CA 92697, USA
[d]Department of Biomedical Engineering, University of California, Irvine, CA 92697, USA
†Electronic supplementary information (ESI) available. See DOI: 10.1039/c4an02244k

no measurable ionic transport is observed[2] or the pore ionic conductance is orders of magnitude lower compared to the case when the pore is filled with condensed water.[4] A sufficiently high magnitude of voltage is needed to push the solution into the pore, which is observed as a sharp increase of the transmembrane current. Subsequent lowering of the applied electric field leads to pore closure interpreted as water evaporation. Interestingly, hysteresis known for pressure driven systems is also prominent in electric field induced wetting: voltage needed to open a pore for ionic transport is higher than the voltage at which evaporation occurs.[1,2,4]

Several mechanisms were suggested for the electric field induced wetting. Electrostriction, *i.e.* electric field induced increase of water density, was theoretically predicted to occur in hydrophobic nanopores and lead to water infiltration.[14–16] Although bulk water is characterized by low compressibility, diminished density of water close to hydrophobic surfaces[17] make it prone to electrostriction. Electrowetting, the electric field induced lowering of the contact angle, was suggested as another mechanism for wetting of low aspect ratio silicon nitride pores.[4] Wetting of hydrophobic nanopores can also be facilitated by water polarizability and the natural tendency of a polar medium to move into zones with high electric fields.

Although wetting of hydrophobic pores by electric field is experimentally achieved using electrolytes and not pure water, the importance of ions for wetting and dewetting processes is not always taken into account or discussed. A set of experiments and calculations performed by Smirnov suggested ionic concentrations had very little influence on the process of wetting of hydrophobic nanopores.[4] Concentration and ion type is however known to be important for hydrophobic interactions as evidenced by experimental studies on the effect of salt on non-polar solutes' solubility.[18–22] Small ions with high charge density were shown to decrease the solute' solubility; the effect of larger ions was the opposite, the presence of salt diminished hydrophobic interactions between solutes. Molecular dynamics simulations by Lu *et al.* revealed that higher pressures would need to be applied to infiltrate a molecular-sized nanopore with a salt solution compared to pressures needed to wet the pore with pure water.[23] Presence of ions in a pore was found to promote dewetting in another molecular dynamics study.[24] An opposite effect was reported as well: presence of ionic concentration gradient was found to promote wetting of nanopores.[12,13] Charge density of ions was also shown to modulate hydrophobic interactions between two parallel plates.[18]

In this manuscript we present experimental results on the effect of salt concentration on hydrophobic gating in single polymer nanopores whose pore walls were modified with alkyl chains of different lengths. Planar surfaces subjected to the same modification as single nanopores showed contact angle below 90 °C, suggesting the surfaces contained regions of hydrophobic and hydrophilic character. Nanopores modified with propyl and hexyl chains could be opened for ionic transport at lower KCl concentrations compared to nanopores modified with decyl molecules. All pores which showed hydro-

phobic gating exhibited modification-independent closed state of less than 5 pA transmembrane current. The results are explained in the context of Maxwell stress and osmotic pressure induced outward stress, which change the shape of the liquid–vapor interface in a salt concentration dependent fashion. We use the model developed by Lee and Kang for a lipid–gas interface present in a nanoslit created by two charged parallel plates.[25]

Experimental methods

Preparation of nanopores

All nanopores used in the presented experiments were prepared in 12 μm thick films of polyethylene terephthalate (PET) by the track-etching technique.[26] The films were first irradiated with single energetic heavy ions at the linear accelerator UNILAC at the Institute for Heavy Ions Research in Darmstadt, Germany.[27] The irradiated films were subjected to etching in 9 M NaOH from one side while the other side of the film was in contact with an acidic stopping medium. This asymmetric etching procedure is known to lead to preparation of conically shaped nanopores.[28] The PET nanopores used in this study had the small opening, the tip, between 5 and 12 nm, and the large opening, called the base, between 300 and 700 nm.

Chemical modification of PET nanopores

Etching of irradiated PET films in NaOH leads to preparation of pores whose walls contain carboxyl groups at the density of 1 per nm^2. These groups provide a convenient route to the attachment of hydrophobic groups to the walls using the coupling agent (*N*-(3-dimethylaminopropyl)-*N*′-ethylcarbodiimide hydrochloride) (EDC). We used propylamine, hexylamine and decylamine whose amine groups were linked with carboxyls on the pore walls creating an amide bond. The two-step procedure described by Ali *et al.* was used.[29] The first step entails 60 min incubation of both sides of a membrane in an ethanol solution of 0.1 M EDC and 0.2 M pentafluorophenol (PFP). The pore was washed carefully with ethanol and in the second step the membrane was incubated with 50 mM propylamine (or hexylamine or decylamine) for 2 hours. After the modification, the pores were carefully washed again with ethanol and subsequently water.

Recordings of ion current

Single pore membranes were examined using the same conductivity cell in which the etching was performed. Current–voltage curves were recorded using two non-polarizable Ag/AgCl electrodes and a 6487 Keithley picoammeter voltage source. The voltage was cycled in the range between −10 V and +10 V in the forward and reversed directions to observe hysteresis. Voltage was changed stepwise and to avoid capacitance effects, each voltage step was held for at least 3 s after which a current value was recorded. Multiple scans allowed calculating average values of the current with standard deviation. A few pores were also examined using 200B Axopatch and 1322A

Digidata (Molecular Devices, Inc.). Ion current signal was recorded at each voltage step for 30 s. Current–voltage curves were obtaining by time averaging of the signals. 10 mM, 0.1 M, and 1 M KCl solutions were buffered to pH 8 with Tris buffer.
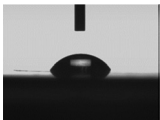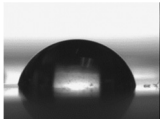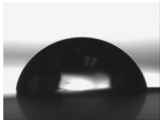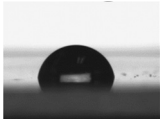
Results and discussion

Fig. 1 presents current–voltage curves recorded in 10 mM, 0.1 M, and 1 M KCl, pH 8, through three sub-10 nm PET pores modified with propylamine, hexylamine and decylamine, respectively. The chemical modifications were achieved by linking the amines with carboxyl groups on the pore walls using EDC-mediated chemistry.[29,30] The amine groups are

used to create an amide bond exposing the alkyl chain to the solution. Table 1 summarizes contact angle values for planar PET surfaces subjected to the same chemical modifications as the single-pore membranes. We found the measured values were similar in water and KCl concentrations in the range between 10 mM and 1 M (not shown). Contact angle is a macroscopic measurement, which predicted only insignificant differences between the three surfaces. All three modifications led to an increased contact angle compared to unmodified PET but measured values below 90° suggest the surfaces consisted of hydrophobic and hydrophilic islands. The presence of unreacted carboxyl groups is also evidenced by the ion current rectification modified pores exhibited, especially pronounced in 100 mM KCl (Fig. 1). Rectification in conically
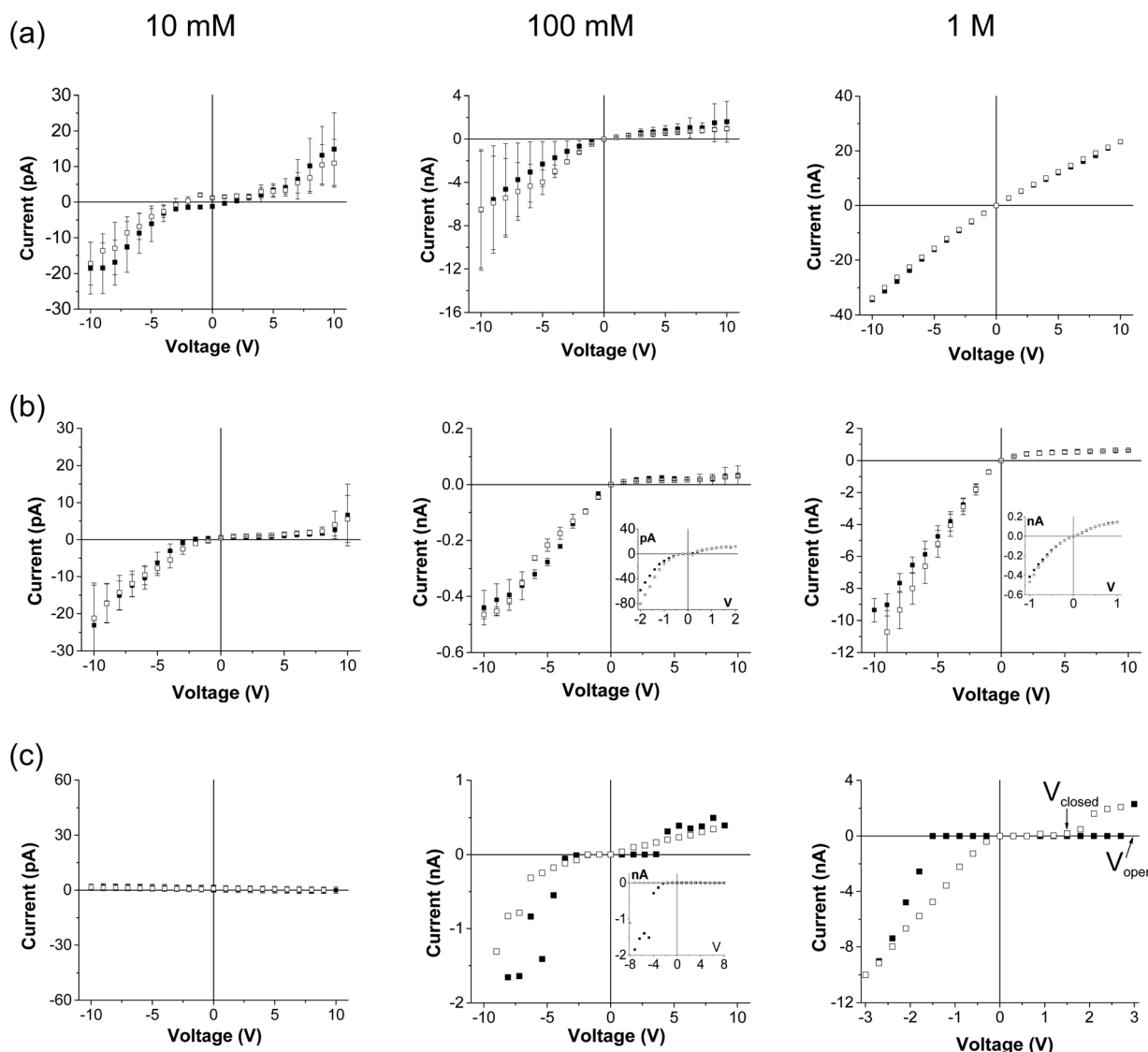
Fig. 1 Current voltage curves through single conically shaped nanopores modified with (a) propylamine, (b) hexylamine, and (c) decylamine. Filled and empty squares indicate forward and reverse bias, respectively. The pore opening diameter was (a) 5 nm, (b) 6 nm, and (c) 9 nm. The recordings were performed in 10 mM, 100 mM and 1 M KCl. Insets in (b) indicate behavior of the same pore at a lower voltage range, performed in addition to the (−10 V, +10 V) scans. Panel (c) 1 M contains a single scan, and a summary of 26 scans is presented in Fig. 2a; two individual scans for 100 mM are shown.

Table 1 Contact angle of etched PET surfaces subjected to the same modification as single nanopores shown in Fig. 1

Modification of PET	Contact angle in water
Unmodified	$58.0° \pm 6.0°$
Propylamine	$76.6° \pm 5.8°$
Hexylamine	$75.0° \pm 3.4°$
Decylamine	$79.4° \pm 4.2°$

shaped nanopores can be observed only if the pore walls contain excess surface charge.[28–38] The direction of rectification after the hydrophobic modification is the same as before the amine attachment pointing to the presence of residual negative charges.[33] These observations are also in agreement with previous reports on the difficulty in achieving complete conversion of surface carboxyls groups using EDC coupling.[39,40]

Although the contact angle of surfaces modified with propyl, hexyl and decylamine was very similar, current–voltage curves of nanopores with the same modifications were different from each other. All pores shown in Fig. 1 exhibited hydrophobic gating i.e. voltage induced switching between non-conducting and conducting states, however the salt concentration and voltage range at which it occurred differed between the three types of pores. The propylamine modified pore showed very low conductance and a weak gating in 10 mM KCl (Fig. 1a): the pore switched between a closed state with currents below 5 pA and a weakly conducting state of just tens of pA. When increasing the salt concentration to 100 mM KCl, the pore became conductive for ions at all examined voltages, and in 1 M KCl, the measured currents were quantitatively very similar to values before the chemical modification. When lowering the salt concentration down to 10 mM KCl, the pore remained conductive, and only subsequent air drying of the sample closed it for ionic transport. Similar behavior was observed with another independently prepared nanopore modified with propylamine (Fig. S1†). Hexylamine modified nanopores remained mostly non-conductive in 10 mM KCl with similar values of the current as for the propylamine nanopore (Fig. 1b, Fig. S2†). In 100 mM KCl the pores switched between non-conducting and conducting states but eventually became conductive for ions at all voltages. No gating was observed in 1 M KCl. The hexylamine modified nanopore

shown in Fig. 1b also exhibited high rectification; we do not have yet explanation for this effect.

The largest number of pores was subjected to the modification with decylamines. 7 pores could not be open for ionic transport even in 1 M KCl and voltage of 10 V. 5 pores conducted current for all KCl concentrations, often with reduced values of current compared to the values before the modification. 7 pores were closed in 10 mM KCl but started to conduct current either in 100 mM or 1 M KCl; these pores exhibited hydrophobic gating thus voltage induced switching between conducting and non-conducting states. We also studied one 11 nm in diameter pore which gated in 10 mM KCl and opened for higher molarities. Fig. 1c shows recordings through a 9 nm pore, which was completely closed in 10 mM KCl, opened for ionic transport in 100 mM KCl for voltages of ~4 V, and exhibited repeatable switching between conductive and non-conductive states for 26 cycles of voltage in 1 M KCl (Fig. 2a). It is important to mention that the recordings in 100 mM KCl were taken before the data in 1 M KCl and 10 mM; this pore was therefore able to undergo dewetting by lowering ionic concentration. The non-conducting state of all hydrophobic devices is attributed to a pore containing at least one vapor pocket, which interrupts water and ionic flow.

We would like to emphasize two unique observations with the decylamine modified nanopore in 1 M KCl (Fig. 1c). The first striking feature was the ability of the pore to reversibly switch between a closed state with currents below 5 pA, and high conductance states of a few nA. This pore also exhibited a well-defined hysteresis such that voltages required to open the pore for ionic transport (V_{open}) were higher than voltages at which the pore stopped conducting (V_{closed}). The hysteresis was present for both voltage polarities. Similar observations were recorded with two other nanopores modified with decylamine in the same conditions as the 9 nm pore shown in Fig. 1c. In order to facilitate comparison of the effect of hydrophobic gating observed with different pores, we summarized the voltage scans by noting the values of voltage V_{open} and V_{closed}. The results for three pores are summarized in Fig. 2. The reproducibility of the values of V_{closed} and V_{open} is especially clear for the pore shown in Fig. 2c, which repeatedly opened and closed for 30 cycles between −5 V and +5 V and an additional 20 cycles in the scans (−4 V, +4 V) (not shown).

Our experiments on nanopores modified with three types of alkyl chains point to the conclusion that higher KCl concentrations promote wetting of the pores. The results are in agreement with experimental and theoretical studies showing that added salts can modulate the strength of hydrogen interactions between water molecules as well as hydrophobic interactions.[18–22] The experimental results also suggest that repeatable gating between conducting and non-conducting states is facilitated by the attachment of a longer alkyl chain to the pore walls (Fig. 1). Even though the three modifications produced surfaces of similar contact angle, nanopores modified with the three molecules exhibited different transport properties and KCl concentration dependence.
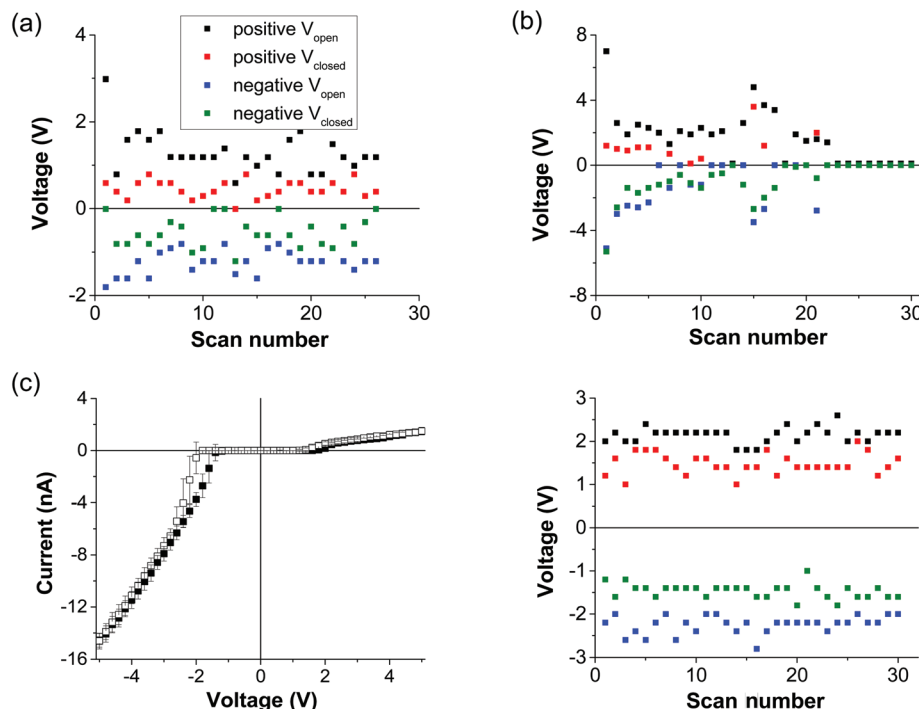
Fig. 2 Hydrophobic gating of three sub-10 nm nanopores modified with decylamine. The pores had opening diameter of (a) 9 nm (the same pore as shown in Fig. 1c), (b) 6 nm, and (c) 6 nm. A summary of voltages at which the pores became conductive in the forward bias (V_{open}), and voltages at which the pores stopped conducting (V_{closed}) is shown. Values for both voltage polarities are plotted. The pore in (b) became conductive for all voltages in 22nd scan. The pore shown in (c) exhibited the most reproducible values of V_{open} and V_{closed} thus the current−voltage curve averaged over 30 scans features very small variability; filled and empty squares indicate forward and reverse bias, respectively.

Another important point to note is that even nanopores modified with propylamine were able to form a closed state with a very small conductance of just a few of pA for few volts. An ability to achieve a completely closed state with modest hydrophobic modifications is in agreement with molecular dynamics modeling performed with surfaces containing hydrophobic and hydrophilic patches.[41–43] The modeling revealed that a patch as small as 2 nm is sufficient to induce water evaporation.

This observation is however in disagreement with an earlier experimental report on hydrophobic gating in chemically modified silicon nitride pores with much large opening diameter of ~100 nm. These pores also switched between closed and open states however conductance of the pores in the closed state was dependent on the type of hydrophobic modification: the closed state resistance was lower for less hydrophobic modifications.[4] Existence of the finite conductance for all voltages was explained by the presence of a water layer at the pore walls and the assumption that the pore was never completely dry.[44] There could be at least two reasons why our hydrophobic nanopores had a closed state with almost zero currents for all chemical modifications. (i) The polymer pores studied in this report are characterized by a high aspect ratio thus the residual surface conductance might produce currents less than 10 pA even at voltages of few volts. (ii) Another possibility could be the truly nanometer scale of the polymer nanopores; water density close to hydrophobic surfaces

might indeed be too low to allow ions to be present close the surface.

A starting point to considering the effect of voltage and salt concentration on transport properties of our nanopores is with equations that have previously been used to explain hydrophobic gating in nanopores. Vlassiouk et al. considered electrostatic pressure that arises from the electrostatic energy of a capacitor created by two water menisci across a vapor pocket:[4]

$$P_{electrostatic} = \varepsilon_0 \frac{E^2}{2} \qquad (1)$$

The critical pressure needed to force influx of water into a pore whose walls are characterized by a contact angle of θ can be estimated from the macroscopic description given by the Young–Laplace equation:

$$\Delta P = \frac{4\gamma \cos \theta}{D} - P_{electrostatic} \qquad (2)$$

where D is the opening diameter of the pore, and γ is surface tension of water.

As mentioned above, we assume walls of our alkyl modified pores consist of hydrophobic and hydrophilic patches. Hydrophobic gating occurs due to the presence of the hydrophobic zones, whose contact angle can be approximated by the value obtained with C10 thiols chemisorbed on a gold layer;[45] the contact angle was measured 113°. Thus, the calculated critical

electric field necessary to open a 10 nm in diameter pore is equal to $\sim 1.6 \times 10^9$ V m^{-1}. Our pores have hydrophobic and hydrophilic zones, thus the closed state of the device will not correspond to the whole 12 μm pore length filled with vapor. Instead, the pore will contain alternating vapor and condensed pockets. If we assume there is only one vapor pocket that is 20 nm long, the voltage needed to wet the pore is ~ 30 V, a much higher value than measured experimentally. If there are multiple vapor pockets the required voltage would be even higher.

As the next step, we considered a model developed by Dzubiella and Hansen[13] that also predicted an existence of a critical electric field needed to fill a hydrophobic nanopore with water. The proposed relationship for the free energy difference between filled and empty states of a nanopore contained the electrostatic energy difference term; different permittivities of confined water and its vapor were assumed. The critical electric field was calculated for the case when the free energy difference became zero. Using similar parameters as these above in eqn (1) and the presence of just one 20 nm long vapor pocket, the derived equation (eqn (9) in ref. 13) predicted a value of required voltage of ~ 20 V.

Vlassiouk et al. considered electrowetting as the mechanism for voltage-dependent opening of their pores.[4] We cannot apply this approach, because our closed state in low voltages and/or KCl concentrations does not have finite ionic conductance. Thus, the pore walls in contact with the vapor pocket might not be wet i.e. the two reservoirs on both sides of the pocket are not electrically connected (Fig. 3).

In order to explain the observed dependence of the wetting process on KCl concentration and applied voltage, we will focus on the residual surface charges on the nanopore walls. Let's consider a nanopore with one vapor pocket flanked by two regions filled with a salt solution (Fig. 3). We will look closely at the outward stress components acting on a surface perpendicular to the pore axis with a focus on the liquid–gas interface. This situation without an externally applied field can be qualitatively described by a model developed for a similar interface present in a nanoslit created by two charged parallel plates separated by a distance of few nm.[25] The electric potential on the plates/pore walls induces ionic selectivity thus the

regions with salt solution will be predominantly filled with counterions. Local concentration of ions and electric potential can be then described by the Poisson–Boltzmann equation. The electric potential has a radial profile, which leads to a non-homogeneous electric field, $E(r)$.

In the absence of fluid flow and gravity effects, the magnitude of the total stress, T_z, on a surface in an electrolyte perpendicular to the slit axis is given by the sum of the osmotic pressure contribution, π, and the Maxwell stress contribution:[25]

$$T_z(r) = \pi + \frac{1}{2}\varepsilon\varepsilon_0 E^2(r) \tag{3}$$

This electromechanical approach to wetting has been applied before when considering electrowetting phenomena with conducting liquids and surfaces.[46] The osmotic pressure can be calculated via free charge density n_f in a solution (difference between concentrations of counterions and co-ions, which fulfills the Gauss equation) and local electric field E: $\nabla \pi = n_f E$.[25,46]

Under the assumption that no osmotic pressure exists in the vapor phase and that the electric permittivity of the gas phase is much lower than that of the salt solution, one can consider only the electrolyte contribution to the outward stress. Due to radial inhomogeneity of the electric field originating from the charged walls, the total outward stress in the z direction, T_z, is a function of r and assumes maximum values close to the walls (Fig. 3). At the liquid–gas interface the presence of T_z leads to electrocapillarity.[25,46,47] It is important to note that only the stress exerted on a surface perpendicular to the pore axis is spatially inhomogeneous. As shown before, the normal stress exerted on a surface parallel to the slit axis is constant across the slit width and equal to the osmotic pressure at the centerline of the slit.[10]

In the case of two parallel plates distant by $2h$ and a limit of low surface potentials, the following analytical formula was derived for the magnitude of the outward pressure in the z-direction:[25]

$$T_z(r) = n_b kT \left(\frac{zeV}{kT}\right)^2 \frac{2\cosh 2\kappa r}{\cosh 2\kappa h + 1} + 2n_b kT \tag{4a}$$

$$V = \frac{\sigma}{\kappa\varepsilon\varepsilon_0} \frac{\cosh \kappa h}{\sinh \kappa h} \tag{4b}$$

where n_b is the concentration of ions in the bulk expressed as number of ions per unit volume, k and T stand for Boltzmann constant and temperature, respectively, κ is the inverse Debye length, V is the surface electric potential on the plates, and σ surface charge density of the plates. Eqn (4) was derived assuming a flat shape of the gas–liquid interface.

T_z as predicted from eqn. (4) for $T = 293$ K, $h = 3$ nm, and $\sigma = 0.02$ C m^{-2} is shown in Fig. 4. Larger magnitudes of T_z close to the walls confirm that conditions for electrocapillarity have indeed been created. Eqn (4) also predicts an increase of the outward stress magnitude with the increase of salt concentration. The shape of liquid–gas interface is therefore modu-
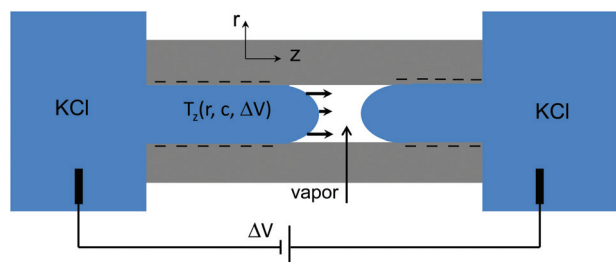
Fig. 3 A scheme of a liquid–vapor interface inside a nanopore. An outward stress in the z-direction, T_z, acting on the interface originates from Maxwell stress and osmotic pressure.[25,46] The radially inhomogeneous electric field leads to radial dependence of the outward stress magnitude and electrocapillarity effect.
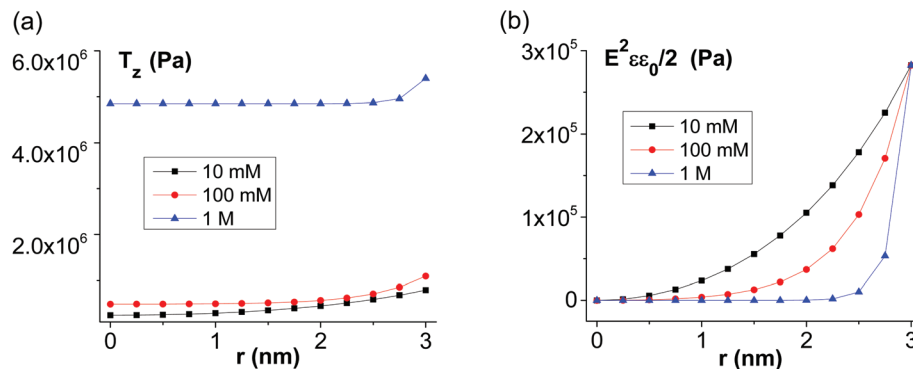
Fig. 4 Outward stress in the z-direction calculated for a nanoslit separated by a distance $2h$ and containing a vapor–liquid interface. The position 0 corresponds to the nanoslit center. (a) Eqn (4) for three bulk KCl concentrations is plotted. (b) Maxwell stress component $\varepsilon_0 \varepsilon E^2/2$ calculated based on eqn (9) and (22) in ref. 25 for a nanoslit. The following parameters were used in the calculations: $\sigma = 0.02$ C m^{-2}, $h = 3$ nm, and $T = 293$ K.

lated by the salt concentration, which explains our experimental observation that some nanopores became conductive to ions by a mere increase of KCl concentration in the bulk electrolyte (Fig. 1a).

Fig. 4b shows the Maxwell stress component calculated using an analytical formula for the radial distribution of the electric field found for the nanoslit.[25] As intuitively predicted, the component is larger in magnitude for more diluted solutions and close to the walls. Fig. 4 also clearly indicates the importance of both contributions, due to osmotic pressure and Maxwell stress, in the development of the total outward stress, T_z, acting on the gas–liquid interface.

Adding external voltage is expected to further increase the outward stress, which will change the shape and position of the liquid–vapor interface, and eventually lead to pore wetting. Our data suggest that pores modified with the longest studied here alkyl chain C10 require both increase of KCl concentration and applied voltage to change the shape of the liquid–vapor interface and cause wetting.

The case of cylindrical geometry, which would be a better model for the experimental system considered here, is more complicated, and we will include it in future work.

According to the mechanism discussed above, the presence of residual surface charges is crucial for the observed salt concentration dependent wetting. SiN pores considered by Vlassiouk *et al.* were characterized with contact angles over 100° and most probably did not contain residual surface charges.[4] As a result, Maxwell stress in their system did not contribute to the wetting process, and no salt concentration dependence of wetting was observed.

We also would like to mention another mechanism which could contribute to the observed salt dependence of hydrophobic gating; this mechanism is not related with the presence of residual charges on the pore walls. Due to the large aspect ratio of considered pores, the so-called access resistance present at pore entrances is typically not taken into account.[48] It is possible however that this additional resistance element could modulate the electric field across vapor pockets. Access resistance increases with the decrease of salt concentration

thus in more diluted solutions a larger portion of the applied voltage will drop at the pore entrance; as a result, the electric field across vapor pocket(s) in a nanopore will be lower. We believe however this mechanism does not dominate in our system since no systematic dependence of the threshold voltage needed to wet a nanopore on pore opening diameters was found.

Conclusions

In this manuscript we present experimental results on transport properties of nanopores that underwent modest hydrophobic modifications by the attachment of C3, C6 and C10 alkyl chains. Although planar surfaces modified according to the same procedures showed similar values of contact angle, nanopores with the shortest alkyl chains exhibited the weakest hydrophobic gating and could be opened for ionic transport already in 10 mM KCl. C10 modified nanopores were mostly closed for ionic transport in 10 mM, but conducted current for voltages above a threshold value in 0.1 M and 1 M KCl; these pores also featured repeatable voltage-induced transitions between conductive and non-conductive states.

Our experiments indicate that modestly hydrophobic nanopores containing hydrophobic and hydrophilic regions on the pore walls exhibit not only voltage but also KCl concentration dependent transport properties. The effect of salt was described by the outward stress component originating from Maxwell stress and osmotic pressure that lead to electrocapillary effect. As a result, the shape of liquid–vapor interface in a charged nanopore is modulated by the presence of local electric fields. The data and the model indicate that contact angle measurement might not be a good predictor of behavior of nanopores at the nanoscale especially for heterogeneous surfaces.

The presented system of nanopores with hydrophobic islands is obtained only when the surface modification of existing surface charges of the pore walls is not complete. The EDC mediated chemistry of linking amines to carboxyls

indeed does not lead to the complete conversion of the surface groups.[39,40] When using another type of chemical modification, one will have to tune the time of the chemical reaction as well as concentration of reagents to assure partial surface modification. This approach was used before when modifying PET pores with (trimethylsilyl) diazomethane.[2]

Finally, it is indeed surprising that nanopores with opening diameters as large as 10 nm exhibit hydrophobic gating. Such wide structures were shown before to exhibit a large kinetic barrier for water evaporation, which would prevent the dewetting process from occurring.[11,15,16,49,50] The results presented here are however in agreement with other experimental reports showing switching between conducting and non-conducting states even with pores having openings of ~100 nm.[4] It was suggested that the presence of residual gases might favor the process of dewetting.[1] We would also like to point to the possibility that flexible polymer chains, which are known to line PET pores,[51] can facilitate dewetting as well. According to the model presented in ref. 52 hydrophobic nanopores whose pore walls can "breathe" favor evaporation; more rigid structures favor water condensation and wetting. This hypothesis could be tested by experimental studies performed with rigid nanopores fabricated e.g. in SiN.

Nanopores which exhibit repeatable opening and closing with voltage could become the basis for drug-delivery systems and ionic circuits. The majority of nanopore based devices focus on controlling transport of ions and molecules.[34] Hydrophobic interactions and hydrophobic gating open a route for preparation of more complete valves which can regulate transport of water and all species that are dissolved in it.[3]

Acknowledgements

Notes and references

1 S. Smirnov, I. Vlassiouk, P. Takmakov and F. Rios, *ACS Nano*, 2010, **4**, 5069–5075.
2 M. R. Powell, L. Cleary, M. Davenport, K. J. Shea and Z. S. Siwy, *Nat. Nanotechnol.*, 2011, **6**, 798–802.
3 U. Rant, *Nat. Nanotechnol.*, 2011, **6**, 759–760.
4 S. N. Smirnov, I. V. Vlassiouk and N. V. Lavrik, *ACS Nano*, 2011, **5**, 7453–7461.
5 O. Beckstein and M. S. P. Sansom, *Proc. Natl. Acad. Sci. U. S. A.*, 2003, **100**, 7063–7068.
6 I. Vlassiouk, C.-D. Park, S. A. Vail, D. Gust and S. Smirnov, *Nano Lett.*, 2006, **6**, 1013–1017.
7 M. H. Factorovich, E. G. Solveyra, V. Molinero and D. A. Scherlis, *J. Phys. Chem. C*, 2014, **118**, 16290–16300.
8 M. Thommes, *Chem. Ing. Technol.*, 2010, **82**, 1059–1073.
9 S. Inagaki and Y. Fukushima, *Microporous Mesoporous Mater.*, 1998, **21**, 667–672.
10 J. N. Israelachvili, *Intermolecular and Surface Forces*, Academic, San Diego, 1991.
11 D. Bratko, C. D. Daub, K. Leung and A. Luzar, *J. Am. Chem. Soc.*, 2007, **129**, 2504–2510.
12 J. Dzubiella, R. J. Allen and J.-P. Hansen, *J. Chem. Phys.*, 2004, **120**, 5001–5004.
13 J. Dzubiella and J.-P. Hansen, *J. Chem. Phys.*, 2005, **122**, 234706.
14 D. Vanzo, D. Bratko and A. Luzar, *J. Chem. Phys.*, 2014, **140**, 074710.
15 D. Bratko, C. D. Daub and A. Luzar, *Faraday Discuss.*, 2009, **141**, 55–66.
16 D. Bratko, C. D. Daub and A. Luzar, *Phys. Chem. Chem. Phys.*, 2008, **10**, 6807–6813.
17 D. A. Doshi, E. B. Watkins, J. Israelachvili and J. Majewski, *Proc. Natl. Acad. Sci. U. S. A.*, 2005, **102**, 9458–9462.
18 R. Zangi, M. Hagen and B. J. Berne, *J. Am. Chem. Soc.*, 2007, **129**, 4678–4686.
19 F. Hofmeister, *Arch. Exp. Pathol. Pharmakol.*, 1888, **XXV**, 1–30.
20 K. D. Collins, *Biophys. J.*, 1997, **72**, 65–76.
21 R. L. Baldwin, *Biophys. J.*, 1996, **71**, 2056–2063.
22 B. Hribar, N. T. Southall, V. Vlachy and K. A. Dill, *J. Am. Chem. Soc.*, 2002, **124**, 12302–12311.
23 L. Liu, X. Chen, W. Lu, A. Han and Y. Qiao, *Phys. Rev. Lett.*, 2009, **102**, 184501.
24 J. Dzubiella and J.-P. Hansen, *Mol. Phys.*, 2013, **111**, 3404–3409.
25 J. A. Lee and I. S. Kang, *Phys. Rev. E: Stat. Phys., Plasmas, Fluids, Relat. Interdiscip. Top.*, 2014, **90**, 032401.
26 R. L. Fleischer, P. B. Price and R. M. Walker, *Nuclear Tracks in Solids: Principles and Applications*, University of California Press, Berkeley CA, 1975.
27 R. Spohr, Methods and Device to Generate a Predetermined Number of Ion Tracks, *German Patent* DE2951376 C2, 15 Sept 1983, US Patent 4369370, 1983.
28 P. Y. Apel, Y. E. Korchev, Z. Siwy, R. Spohr and M. Yoshida, *Nucl. Instrum. Methods Phys. Res., Sect. B*, 2001, **184**, 337–346.
29 M. Ali, V. Bayer, B. Schiedt, R. Neumann and W. Ensinger, *Nanotechnology*, 2008, **19**, 485711.
30 G. Nguyen, I. Vlassiouk and Z. S. Siwy, *Nanotechnology*, 2010, **21**, 265301.
31 C. Wei, A. J. Bard and S. W. Feldberg, *Anal. Chem.*, 1997, **69**, 4627–4633.
32 Z. Siwy and A. Fulinski, *Phys. Rev. Lett.*, 2002, **89**, 198103.
33 Z. S. Siwy, *Adv. Funct. Mater.*, 2006, **16**, 735–746.

34 Z. S. Siwy and S. Howorka, *Chem. Soc. Rev.*, 2010, **39**, 1115–1132.

35 S. Umehara, N. Pourmand, C. D. Webb, R. W. Davis, K. Yasuda and M. Karhanek, *Nano Lett.*, 2006, **6**, 2486–2492.

36 J. Cervera, B. Schiedt and P. Ramirez, *Europhys. Lett.*, 2005, **71**, 35–41.

37 Z. Siwy, E. Heins, C. C. Harrell, P. Kohli and C. R. Martin, *J. Am. Chem. Soc.*, 2004, **126**, 10850–10851.

38 H. S. White and A. Bund, *Langmuir*, 2008, **24**, 2212–2218.

39 I. Vlassiouk, T. R. Kozel and Z. S. Siwy, *J. Am. Chem. Soc.*, 2009, **131**, 8211–8220.

40 S. Sam, *et al.*, *Langmuir*, 2009, **26**, 809–814.

41 N. Giovambattista, P. G. Debenedetti and P. J. Rossky, *J. Phys. Chem. C*, 2007, **111**, 1323–1332.

42 G. O. F. Parikesit, E. X. Vrouwe, M. T. Blom and J. Westerweel, *Biomicrofluidics*, 2010, **4**, 044103.

43 T. Koishi, K. Yasuoka, T. Ebisuzaki, S. Yoo and X. C. Zeng, *J. Chem. Phys.*, 2005, **123**, 204707.

44 I. Vlassiouk, F. Rios, S. A. Vail, D. Gust and S. Smirnov, *Langmuir*, 2007, **23**, 7784–7792.

45 M. Pevarnik, K. Healy, M. Davenport, J. Yenand and Z. S. Siwy, *Analyst*, 2012, **137**, 2944–2950.

46 F. Mugele and J.-C. Baret, *J. Phys.: Condens. Matter*, 2005, **17**, R705–R774.

47 J. W. van Honschoten, N. Brunets and N. R. Tas, *Chem. Soc. Rev.*, 2010, **39**, 1096–1114.

48 J. E. Hall, *J. Gen. Phys.*, 1975, **66**, 531–532.

49 A. Luzar, *J. Phys. Chem. B*, 2004, **108**, 19859–19866.

50 K. Lum and D. Chandler, *Int. J. Thermophys.*, 1998, **19**, 845–855.

51 E. R. Cruz-Chu, T. Ritz, Z. S. Siwy and K. Schulten, *Faraday Discuss.*, 2009, **143**, 47–62.

52 O. Beckstein and M. S. P. Sansom, *Phys. Biol.*, 2004, **1**, 42–52.